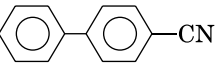
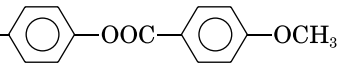
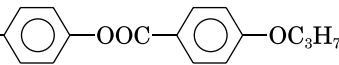
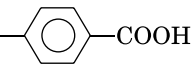
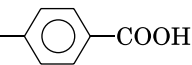
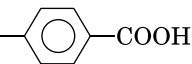
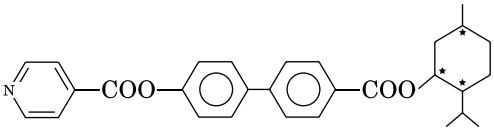


Table I. The Transition Temperatures of Monomers and Chiral Dopant

Name	Chemical Structure	Phase Behavior (°C)
M1	$\text{CH}_2=\text{CH}-\text{COO}-(\text{CH}_2)_4-\text{O}-$ 	K 93 I
M2	$\text{CH}_2=\text{CH}-\text{COO}-(\text{CH}_2)_5-\text{COO}-$ 	K 82 I (N 53 I)
M3	$\text{CH}_2=\text{CH}-\text{COO}-(\text{CH}_2)_5-\text{COO}-$ 	K 66 I (N 55 I)
A3	$\text{CH}_2=\text{CH}-\text{COO}-(\text{CH}_2)_3-\text{O}-$ 	K 109 I (N 103 I)
A6	$\text{CH}_2=\text{CH}-\text{COO}-(\text{CH}_2)_6-\text{O}-$ 	K 85 SmA 96 N 103 I
A9	$\text{CH}_2=\text{CH}-\text{COO}-(\text{CH}_2)_9-\text{O}-$ 	K SmA 97 N 105 I
Mt		K 115-116 I $[\alpha]_D^{22} = -32.4^\circ$, $[M] = -148^\circ$

4'-methoxybenzoate (M2), 4-(6-acryloyloxyhexyl)oxybenzoate (M3), 4-(6-acryloyloxypropyl-1-oxy)-benzoic acid (A3), 4-(6-acryloyloxyhexyl-1-oxy)-benzoic acid (A6), 4-(6-acryloyloxynonyl-1-oxy)-benzoic acid (A9), and chiral dopant 1-menthyl-4-(4-pyridyl)oxybiphenyl-4'-carboxylate (Mt) were synthesized according to the earlier described procedures^{38-41,43} (Table I).

M1

¹H-NMR (CDCl₃): δ 7.97 (d, 2H, Ph, *J* = 8.85 Hz); 7.67 (d, 2H, Ph, *J* = 8.55 Hz); 7.62 (d, 2H, Ph, *J* = 8.51 Hz); 7.51 (d, 2H, Ph, *J* = 8.81 Hz); 6.35 (dd, 1H, CH₂=CH—, *J* = 1.65; 17.65 Hz); 6.12 (dd, 1H, CH₂=CH—, *J* = 10.3; 17.31 Hz); 5.81 (dd, 1H, CH₂=CH—, *J* = 1.65; 10.3 Hz); 4.21 (t, 2H, O—CH₂—); 4.02 (t, 2H, —CH₂—O); 1.89 (4H, —CH₂—CH₂—).

M2

¹H-NMR (CDCl₃): δ 8.12 (d, 2H, Ph); 7.20 (d, 2H, Ph); 7.11 (d, 2H, Ph); 6.95 (d, 2H, Ph); 6.35 (dd, 1H, CH₂=CH—, *J* = 1.65; 17.65 Hz); 6.12 (dd,

1H, CH₂=CH—, *J* = 10.3; 17.31 Hz); 5.81 (dd, 1H, CH₂=CH—, *J* = 1.65; 10.3 Hz); 4.15 (t, 2H, COO—CH₂—); 3.98 (s, 3H, —CH₃); 2.55 (t, 2H, —CH₂—COO); 1.4–1.9 (6H, —CH₂—).

M3

¹H-NMR (CDCl₃): δ 8.12 (d, 2H, Ph); 7.20 (d, 2H, Ph); 7.11 (d, 2H, Ph); 6.95 (d, 2H, Ph); 6.35 (dd, 1H, CH₂=CH—, *J* = 1.65; 17.65 Hz); 6.12 (dd, 1H, CH₂=CH—, *J* = 10.3; 17.31 Hz); 5.81 (dd, 1H, CH₂=CH—, *J* = 1.65; 10.3 Hz); 4.15 (t, 2H, COO—CH₂—); 3.95 (t, 2H, O—CH₂—CH₂—); 2.55 (t, 2H, —CH₂—COO); 1.4–1.9 (8H, —CH₂—); 1.05 (t, 3H, —CH₂—CH₃).

A3

¹H-NMR (CDCl₃): δ 7.95 (d, 2H, Ph, *J* = 8.82 Hz); 6.93 (d, 2H, Ph, *J* = 8.82 Hz); 6.35 (dd, 1H, CH₂=CH—, *J* = 1.65; 17.65 Hz); 6.12 (dd, 1H, CH₂=CH—, *J* = 10.3; 17.31 Hz); 5.81 (dd, 1H, CH₂=CH—, *J* = 1.65; 10.3 Hz); 4.3 (t, 2H, O—CH₂—); 4.12 (t, 2H, —CH₂—O); 2.13 (2H, —CH₂—).

A6

$^1\text{H-NMR}$ (CDCl_3): δ 7.95 (d, 2H, Ph, $J = 8.82$ Hz); 6.93 (d, 2H, Ph, $J = 8.82$ Hz); 6.35 (dd, 1H, $\text{CH}_2=\text{CH}-$, $J = 1.65$; 17.65 Hz); 6.12 (dd, 1H, $\text{CH}_2=\text{CH}-$, $J = 10.3$; 17.31 Hz); 5.81 (dd, 1H, $\text{CH}_2=\text{CH}-$, $J = 1.65$; 10.3 Hz); 4.3 (t, 2H, $\text{O}-\text{CH}_2-$); 4.12 (t, 2H, $-\text{CH}_2-\text{O}$); 1.3–1.9 (8H, $-\text{CH}_2-$).

A9

$^1\text{H-NMR}$ (CDCl_3): δ 7.95 (d, 2H, Ph, $J = 8.82$ Hz); 6.93 (d, 2H, Ph, $J = 8.82$ Hz); 6.35 (dd, 1H, $\text{CH}_2=\text{CH}-$, $J = 1.65$; 17.65 Hz); 6.12 (dd, 1H, $\text{CH}_2=\text{CH}-$, $J = 10.3$; 17.31 Hz); 5.81 (dd, 1H, $\text{CH}_2=\text{CH}-$, $J = 1.65$; 10.3 Hz); 4.31 (t, 2H, $\text{O}-\text{CH}_2-$); 4.12 (t, 2H, $-\text{CH}_2-\text{O}$); 1.2–1.9 (14H, $-\text{CH}_2-$).

Copolymers were obtained by radical copolymerization of monomers M1, M2 with A6, and M3 with A3, A6, A9, respectively, in absolute THF at 60–70°C; AIBN was used an initiating agent. The as-synthesized copolymers were purified by repeated reprecipitation from THF solutions by hexane. Copolymers are soluble in THF and in hot ethanol.

The composition of the copolymers was determined by NMR spectroscopy (see below).

The blends of the copolymers with the pyridine-containing chiral additive were prepared by dissolution of their mechanical mixtures with various compositions in THF and drying in vacuum.

Phase transitions in the synthesized copolymers were studied by differential scanning calorimetry (DSC), with a scanning rate of 10 K/min. The phase-transition temperatures are given as endothermic maxima of the heating curves at the same rate in air. Glass transition temperatures were taken as points of inflexion.

All experiments were performed using a Mettler TA-400 thermal analyzer and a LOMO P-112 polarization microscope with a Mettler FP-80 hot stage. A selective light reflection of chiral polymers was studied with an Hitachi U-3400 UV-VIS-IR spectrometer equipped with a Mettler FP-80 hot stage. The 20 μm -thick samples were sandwiched between the two flat glass plates. The thickness of the test samples was preset by Teflon spacers. Planar texture was obtained by shear deformation of the samples, which were heated to temperatures above the glass transition temperature. Prior to tests, the test samples were annealed for 20–40 min. X-ray diffraction analysis

was carried out using an URS-55 instrument (Ni-filtered CuK_α radiation). Orientation of the polymers for X-ray diffraction studies was performed by slow cooling of the samples in the form of the fibers from isotropic melt to room temperature.

Relative molecular weights of polymers were determined by gel permeation chromatography (GPC) using a GPC-2 Waters instrument equipped with an LC-100 column oven and a Data Modul-370 data station. Measurements were made by using a UV detector, THF as solvent (1 mL/min, 25°C), a set of PL columns of 100, 500, and 10³ Å, and a calibration plot constructed with polystyrene standards.

RESULTS AND DISCUSSION

A well-known traditional method for the preparation of chiral nematic phases is based on covalent binding of chiral molecules to side fragments of the nematic comb-shaped polymers.⁴²

One of the ways to accomplish this binding is copolymerization of a nematogenic monomer (the corresponding homopolymer forms nematic phase) with the monomer containing one or several asymmetric carbon atoms that are responsible for the development of a twisted structure in the copolymer.

In this work, the chiral nematic phase was prepared by an alternative approach, that is, an introduction of a noncovalently bonded low molecular mass chiral dopant to a nematic polymer matrix containing functional carboxylic groups.

Hence, the first stage of this work involves synthesis of the LC copolymers (matrix), which satisfy the following criteria. First, this copolymer should form the nematic phase; second, it should contain a high content of carboxylic groups (not less than 20 mol %), which are necessary for the formation of hydrogen bonds with pyridinium fragment of a chiral additive. Let us consider the properties of the synthesized copolymers.

Phase Behavior of Copolymers

The composition of copolymers was determined by NMR spectroscopy, comparing integral intensity of aromatic protons of a mesogenic group and an oxybenzoic ring. An example of an NMR spectrum for the C₂ copolymer is presented on Figure 1.

Investigating copolymer compositions we have found that the copolymer compositions practically

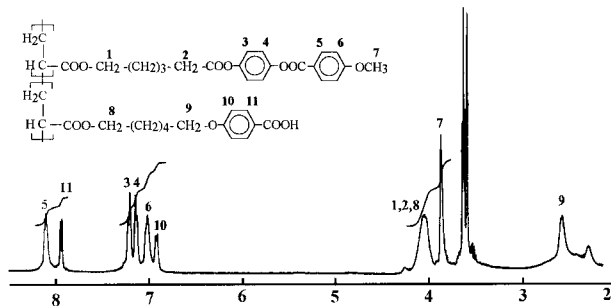


Figure 1. $^1\text{H-NMR}$ spectrum of copolymer C_2 .

do not differ from a composition of the initial monomer mixtures.

Optical microscopic and X-ray studies showed that all synthesized polymers are able to develop a nematic phase (Table II). Upon cooling from the isotropic melt, copolymers form a marble texture, which is a specific property of the nematic phase, and is preserved up to room temperature. The corresponding X-ray patterns of the copolymers show only a diffuse halo at wide scattering angles ($D = 4.6\text{--}4.9 \text{ \AA}$), and the DSC scans exhibit a single endothermic peak with a fusion heat in the range of $\Delta H = 1.3\text{--}1.9 \text{ J/g}$ (depending on the type of copolymers) (Fig. 2), which is associated with the transition from the nematic liquid crystal to the isotropic melt.

Hence, all synthesized copolymers satisfied criteria presented above, and could be used as a nematogenic matrix.

The Influence of the Polymer Matrix on the Properties of the Blends

Phase Behavior of the Blends

Let us consider the phase state of copolymers C_1 , C_2 , and C_3 with the chiral additive Mt. Figure

Table II. The Transition Temperatures and Molecular Mass Characteristics of LC Copolymers

Name	M_n	M_w	M_w/M_n	Phase Transitions/ $^{\circ}\text{C}$
C_1	3300	5000	1.5	g 30 N 88 I
C_2	3800	5700	1.5	g 15 N 90 I
C_3	3700	5000	1.3	g 12 N 94 I
C_4	3600	5400	1.5	N 106 I
C_5	3400	4800	1.4	N 100 I

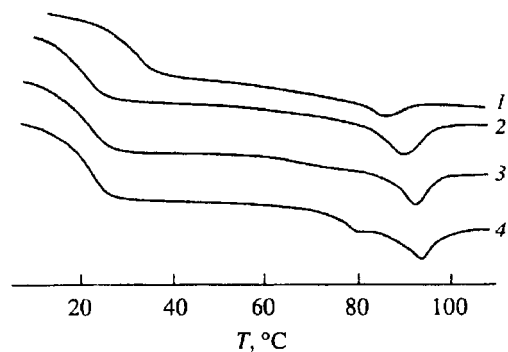


Figure 2. DSC curves for the copolymers C_1 (1), C_3 (2), and for chiral mixtures $C_2\text{-Mt-}5.6$ (3), $C_3\text{-Mt-}11$ (4).

3(a)–(c) shows the phase diagrams of the corresponding blends. The development of the nematic phase is observed for the $C_1\text{-Mt}$ blend in the whole concentration range, while for the $C_2\text{-Mt}$ and $C_3\text{-Mt}$ blends only at a low content of the chiral additive (up to 8.5 and 2.8 mol % of Mt, respectively). In the case of the $C_2\text{-Mt}$ (11.0–21.0 mol % of Mt) and $C_3\text{-Mt}$ (5.6–16.1 mol % Mt) blends, the corresponding DSC curves show two poorly resolved peaks with the total fusion heat of $\sim 3 \text{ J/g}$. This fact probably suggests the development of not only a nematic but also of a smectic phase.

The corresponding X-ray patterns of the above copolymers show two reflections. One X-ray diffuse reflection corresponds to interplanar distance $D = 4.8 \text{ \AA}$, two other reflections correspond to $d_1 = 29.8 \text{ \AA}$ and $d_2 = 16.3 \text{ \AA}$ (for the $C_3\text{-Mt-}16.1$ —the number corresponds to concentration of Mt-dopant, mol %—blend). The presence of small-angle reflections in the X-ray patterns of the blends and a fan-shaped texture observed by an optical microscope suggests the development of an S_A phase. As the concentration of the chiral additive in the $C_3\text{-Mt}$ blends (22.3–32.1 mol % Mt) is increased, the nematic phase disappears, and development of the S_A phase is observed in the whole temperature interval of the mesophase. This evidence is confirmed by the development of the batonnets texture, which is typical of an S_A phase upon cooling from the isotropic melt.

Note that, as evidenced by polarization optical studies, the above nematic phases are helical. Upon cooling from the isotropic melt, one may observe the development of a planar texture with

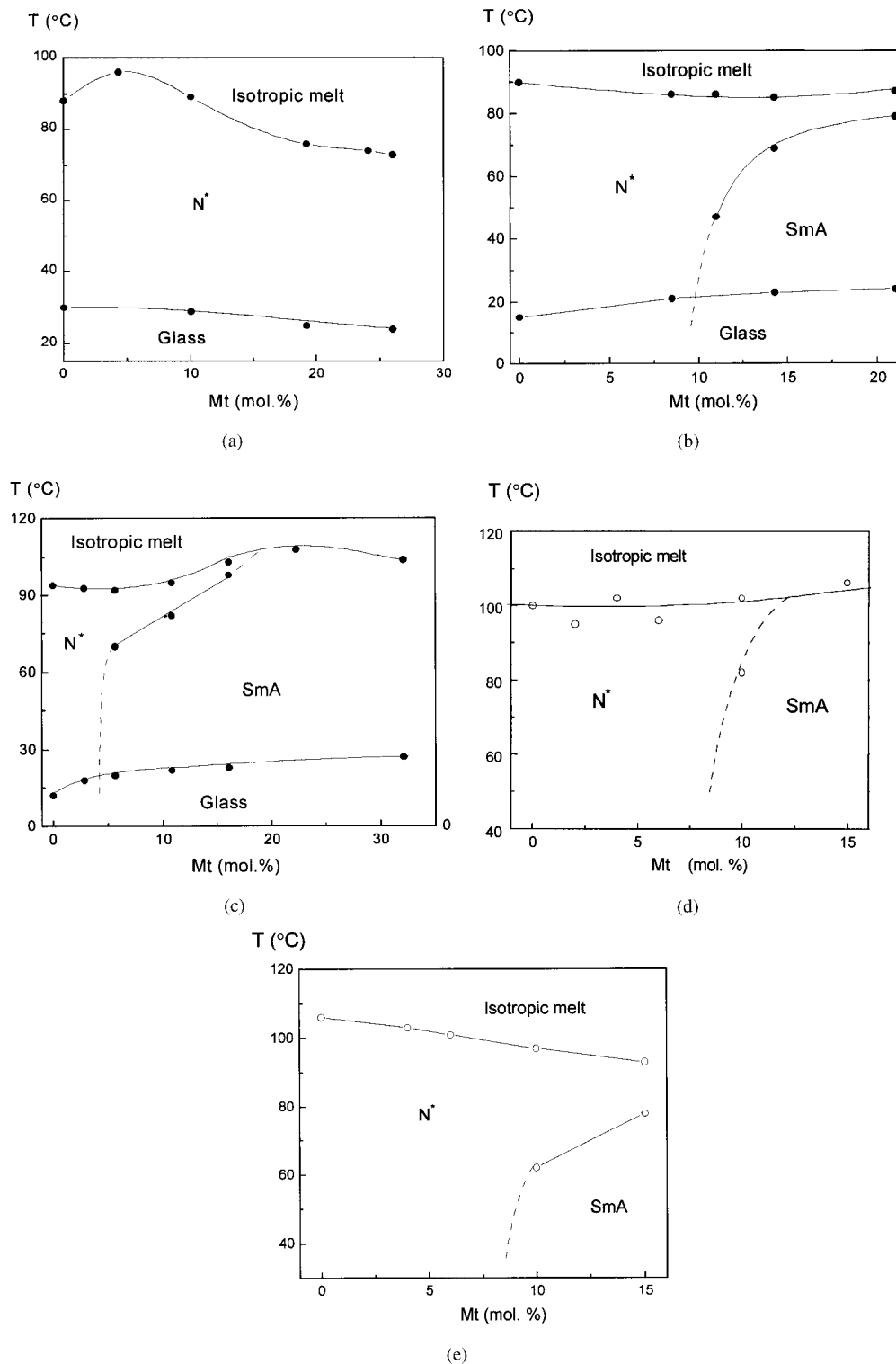


Figure 3. Phase diagrams for the chiral mixtures: (a) C_1 -Mt, (b) C_2 -Mt, (c) C_3 -Mt, (d) C_4 -Mt, (e) C_5 -Mt.

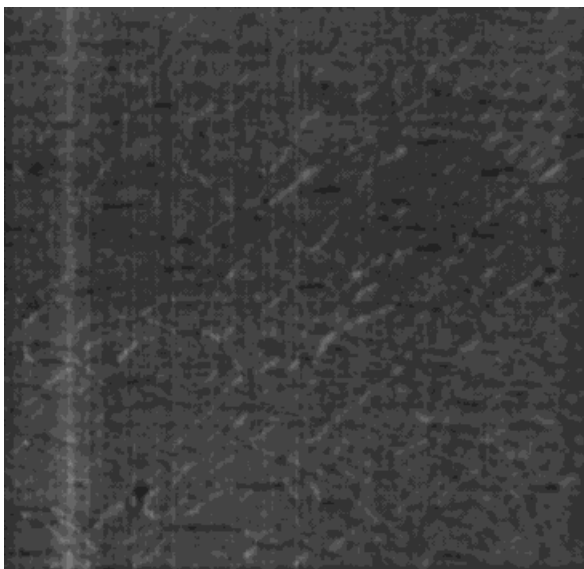
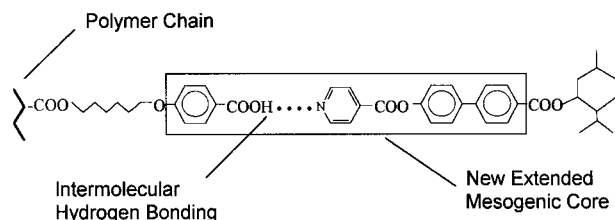


Figure 4. Optical polarizing photomicrograph of blend C₃-Mt-6% (N*, 75°C).

oily streaks, which is typical of the chiral nematic phase (Fig. 4).

Hence, examination of the phase state of three sets of copolymers shows that, upon mixing nematic copolymers containing the crystalline chiral additive Mt, thermodynamically stable blends without any phase separation are produced.

Usually, introduction of nonmesogenic chiral additives dissolved in the nematic mesophase leads to the depression of phase transition temperatures. However, the situation dramatically changes when any additional intermolecular interactions between the nematic matrix and the chiral additive are possible.³⁻⁵ Schematic representation of hydrogen bonds between the monomer fragment of the alkyloxybenzoic acid A6 and the chiral additive Mt is presented below.



The energy of the hydrogen bond between carboxylic acids and pyridines is characterized by high values of $\Delta H \sim 45$ kJ/mol,⁴⁴ which are asso-

ciated with a rigid fixation of the two components in the blend.

Hence, the formation of a new mesogenic fragment with a rod-like shape should increase the clearing temperature of the blends. However, as the fractional content of the chiral molecules is increased, the phase transition temperatures of the C₁-Mt blends slightly decrease, and the T_g of the C₂-Mt and C₃-Mt blends slightly increase. An anticipated improvement in thermal stability of the blends is likely to be compensated by a destabilizing effect of the chiral additive containing a bulky defect, that is, a menthyl group.

Optical Properties of the Blends

Figure 5 shows the transmission spectra of the samples with planar orientation. On average, selective light reflection half-width is changed in the range from 50 to 100 nm. The same values of half-width are typical for previously described menthyl-containing copolymers.^{38,41}

It is noteworthy that all prepared copolymer blends are thermodynamically stable systems. A prolonged keeping of the samples (several weeks) at 50°C does not lead to crystallization of a low molecular mass chiral additive Mt. To prove a marked role of hydrogen bonds in the formation of

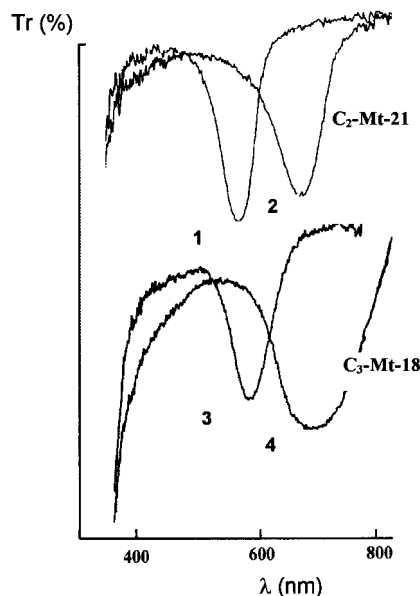


Figure 5. Transmittance spectra for blends: C₂-Mt containing 21 mol % of chiral groups (1, 2) at 83 (1) and 80°C (2); C₃-Mt containing 18 mol % of chiral groups (3, 4) at 70 (3) and 60°C (4).

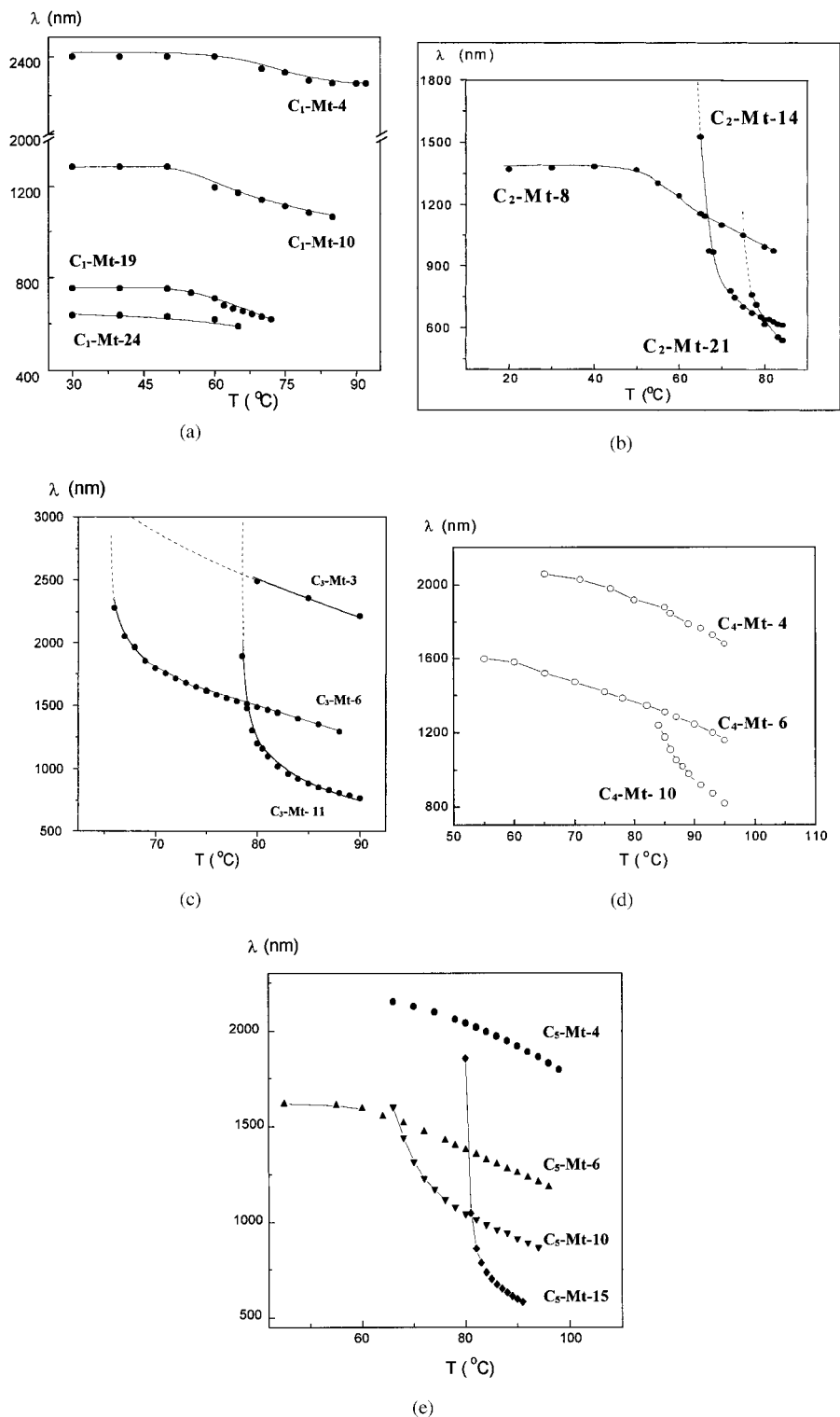
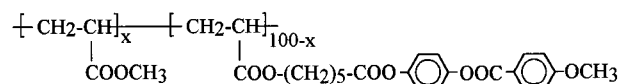


Figure 6. Temperature dependence of the maximum of a selective light reflection for blends C_1 -Mt (a), C_2 -Mt (b), C_3 -Mt (c), C_4 -Mt (d), C_5 -Mt (e).

the blends without phase separation, we prepared blends of Mt with the following LC copolymer containing 39 mol % of methacrylate:



Similar to the C₂ copolymer, this copolymer produces a nematic phase with a clearing temperature of 92°C. When the blend containing 12 mol % of Mt is annealed, phase separation and development of crystals of Mt is observed within 30–40 min. Hence, the absence of any additional noncovalent interactions leads to phase separation of the polymer blend and, as a result, such a blend cannot be used as stable optically active material.

Figures 6(b) and (c) shows the temperature dependences of a maximum selective light reflection wavelength. Upon cooling, selective reflection peak shifts to a long-wavelength region, and this shift is associated with enhanced fluctuations of a smectic order with decreasing temperature and with approaching the nematic–smectic phase transition. Earlier, this behavior was usually observed for cholesterol-containing copolymers⁴⁵ and for copolymers with three-ring menthyl fragments.^{38,41}

The effect of temperature on the helix pitch is most pronounced for the C₃–Mt blends. For the blends containing 11 mol % of the chiral component, as the temperature is decreased by 10°C, maximum selective light reflection wavelength increases by a factor of 3 [Fig. 6(c)].

Helix twisting power (HTP) is an important parameter that characterizes the ability of chiral additive to induce a helical supramolecular structure.^{46,47} To calculate the helix twisting power, A , reciprocal selective light reflection wavelength (at reduced temperature $T = 0.98 T_g$) was plotted against the molar fraction of the chiral component X . Figure 7 shows the typical dependences of $\lambda_{\text{max}}^{-1}$ on X . Helix twisting power was calculated by approximating experimental data through the following function:^{38,41}

$$\lambda_{\text{max}}^{-1} = AX/(1 + BX),$$

where B is the parameter that characterizes the deviation from the linear curve. Parameter B may be associated with a decrease in the order of parameter N^* of the mesophase, or with the presence of the elements of the smectic order.^{38,48}

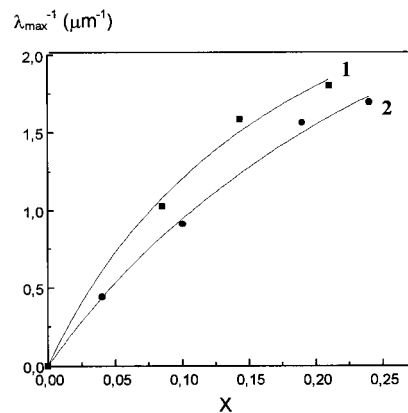


Figure 7. Dependence of $\lambda_{\text{max}}^{-1}$ on the molar fraction of chiral units X : C₂–Mt (1) and C₁–Mt (2).

Table III summarizes the values of A and B for all blends investigated. Analysis of these data allows one to reveal the effect of copolymers nature on helix twisting power of the chiral additive. For example, maximum values of helix twisting power were obtained for the blends of Mt with the copolymer C₂, somewhat lower values were obtained for the C₃–Mt blend; the cyanobiphenyl matrix is characterized by minimum values of twisting power of Mt (Table III).

The Influence of a Distance between the Chiral Dopant and the Main Polymer Chain on Properties of the Blends

Our next goal was to investigate how a distance between the chiral component and the main polymer chain influence on optical properties of the blends.

Let us, first, compare the phase state of copolymers C₃, C₄, C₅ with the chiral additive Mt. The development of the nematic phase is observed for the C₃–Mt, C₄–Mt, and C₅–Mt blends at low content of the chiral additive (up to 3, 10, and 10 mol

Table III. Helical Twisting Power A and Parameter B for the Blends Obtained

Name	$A/\mu\text{m}^{-1}$	B
C ₁ -Mt	12.1 ± 1.1	2.8 ± 0.7
C ₂ -Mt	18.3 ± 1.1	5.5 ± 1.0
C ₃ -Mt	17.3 ± 0.8	4.1 ± 0.7
C ₄ -Mt	19.6 ± 0.5	7.2 ± 0.5
C ₅ -Mt	15.1 ± 1.3	2.2 ± 0.9

% of Mt, respectively) [Fig. 3(c)–(3)]. In the case of C_3 -Mt with a further increase of chiral additive concentration (more than 5%) the nematic phase is substituted by SmA, while the C_4 -Mt blend is able to form a nematic phase up to 20% of the dopant. It is noteworthy that the C_5 -Mt blend does not lose its ability to form a chiral nematic phase in all concentration intervals studied (up to 15 mol %). Analyzing this data one can assume that an increase of a spacer length between the chiral unit and the main polymer chain provides higher stability of the nematic phase.

Figure 6(d) and (e) shows the temperature dependence of a maximum selective light reflection wavelength for C_4 and C_5 blends. Upon cooling, selective reflection peak shifts to a long-wavelength region, and, as mentioned above, this shift is associated with enhanced fluctuations of a smectic order with decreasing temperature and with approach of the nematic–smectic phase transition.

To understand the influence of a distance between the chiral dopant and the main polymer chain on the optical properties of the blends, one should compare values of the helix twisting power (A) (Table III) in the row of C_4, C_3, C_5 copolymers. Copolymers of this row differ from each other only in the length of the flexible spacer, which connects the functional carboxyl group with a main chain. Hence, optical properties of their blends with the dopant Mt will depend only on the spacer length, while the nematic matrix is the same.

From a theoretical consideration of the chiral nematic phase in comb-shaped LC polymers it follows that the helix twisting power depends on two order parameters:

$$S = \frac{1}{2}(3 \cos^2\theta - 1) \quad (1)$$

$$D = \cos 2\psi \quad (2)$$

(where, ψ is an angle of chiral molecule rotation along its long axis) and with increase of this order parameters the helix twisting power is growing.⁴⁹ Finkelmann and Rehage were the first to show that a decrease in the spacer length between the rigid mesogenic group and the main polymer chain leads to higher values of parameter D and an increase of the helix twisting power.⁵⁰ The analogous situation should realize when changing distance between the chiral group and the main polymer chain, the longer distance corresponds to

a lower D , because of a higher “freedom” of the chiral group.

Analysis of our experimental data (Table III) confirms that the same effects control the optical properties of blends with a noncovalently bonded chiral compound, with an decrease of the spacer length (of a distance between the chiral dopant and the main chain) the helix twisting power is increasing. Hence, a flexible alkyl spacer decreases the influence of a chiral compound on the nematic polymer matrix and the longer spacer, a lower the influence.

The values of parameter B are also decreasing in C_4, C_3, C_5 row. This can be explained by enhancing mobility of a bulky menthyl group with respect to the polymer chain with the increase of a spacer length. Hence, winning in the values of a helix twisting power one loses with the high value of parameter B .

The analogous properties of well-known covalent- and noncovalent-bonded polymer chiral systems investigated by us once more prove that chiral additive forms a stable complex with carboxyl functional groups of a polymeric matrix, and due to this, a chiral nematic phase is achieved.

CONCLUSIONS

1. A family of new hydrogen-bonded complexes based on comb-shaped nematic LC copolymers containing the fragments of alkyloxy-4-oxybenzoic acids and a chiral molecule, derivative of 4-pyridinecarboxylic acid, was prepared.
2. At concentrations of chiral groups 1–25 mol %, development of a cholesteric phase is observed. Temperature dependences of a selective light reflection wavelength were studied, and helix twisting power was calculated. Depending on the type of polymer nematic matrix, this value is equal to 12.1–19.6 μm^{-1} . We have shown that an increase of a distance between the chiral dopant and the main polymer chain results in lower values of helix twisting power.
3. With respect to optical properties, the chiral nematic phase in the hydrogen-bonded complexes is comparable to classical cholesteric copolymers, in which the chiral group is covalently bonded to the polymer chain.

REFERENCES AND NOTES

- Kato, T.; Frechet, M. J. *Macromolecules* 1989, 22, 3818.
- Kato, T.; Frechet, M. H. *J Am Chem Soc* 1989, 111, 8533.
- Kato, T.; Frechet, M. J. *Macromol Symp* 1995, 98, 311.
- Bazuin, C. G. In *Mechanical and Thermophysical Properties of Polymer Liquid Crystals*; Chapman & Hall: London, 1998, p. 59, vol. 3.
- Paleos, C. M.; Tsiourvas, D. *Angew Chem Int Ed Engl* 1995, 34, 1696.
- Kresse, H.; Szulzewsky, I.; Diele, S.; Paschke, R. *Mol Cryst Liq Cryst* 1994, 238, 13.
- Lin, H.-C.; Lin, Y.-S. *Liq Cryst* 1998, 24, 315.
- Goldmann, D.; Dietel, R.; Janietz, D.; Schmidt, C.; Wendorff, J. H. *Liq Cryst* 1998, 24, 407.
- Kato, T.; Kihara, H.; Kumar, U.; Fujishima, A.; Uryu, T.; Frechet, J. M. J. *Polymer Preprints* 1993, 34, 722.
- Kumar, U.; Kato, T.; Frechet, J. M. J. *J Am Chem Soc* 1992, 4, 6630.
- Kumar, U.; Frechet, J. M. J.; Kato, T.; Ujiie, S.; Timura, K. *Angew Chem Int Ed Engl* 1992, 31, 1531.
- Kato, T.; Hirota, N.; Fujishima, A.; Frechet, J. M. J. *J Polym Sci Part A* 1996, 34, 57.
- Malik, S.; Dhal, P. K.; Mashelkar, R. A. *Macromolecules* 1995, 28, 2159.
- Sato, A.; Kato, T.; Uryu, T.; *J Polym Sci Part A* 1996, 34, 503.
- Kato, T.; Nakano, M.; Moteki, T.; Uryu, T.; Ujiie, S. *Macromolecules* 1995, 28, 8875.
- Kosaka, Y.; Uryu, T. *Macromolecules* 1994, 27, 6286.
- Kihara, H.; Kato, T.; Uryu, T. *Transact Mater Res Soc Jpn* 1996, 20, 327.
- Kihara, H.; Kato, T.; Uryu, T.; Frechet, J. M. J. *Liq Cryst* 1998, 24, 413.
- St. Pourcain, C. B.; Griffin, A. C. *Macromolecules* 1995, 28, 4116.
- Tsiourvas, D.; Paleos, C. M.; Skoulios, A. *Macromolecules* 1997, 30, 7191.
- Ujiie, S.; Iimura, K. *Chem Lett* 1990, 995.
- Ujiie, S.; Iimura, K. *Chem Lett* 1991, 411.
- Ujiie, S.; Iimura, K. *Macromolecules* 1992, 25, 317.
- Ujiie, S.; Tanaka, Y.; Iimura, K. *Mol Cryst Liq Cryst* 1993, 225, 339.
- Wiesemann, A.; Zentel, R.; Pakula, T. *Polymer* 1992, 33, 5315.
- Bazuin, C. G.; Brandys, F. A.; Eve, T. M.; Plante, M. *Macromol Symp* 1994, 84, 183.
- Bazuin, C. G.; Tork, A. *Macromolecules* 1995, 28, 8877.
- Talroze, R. V.; Plate, N. A. *Polym Sci Ser A* 1994, 36, 1766.
- Talroze, R. V.; Kuptsov, S. A.; Sycheva, T. I.; Bezborodov, V. S.; Plate, N. A. *Macromolecules* 1995, 28, 8689.
- Gohy, J. P.; Vanhoorne, P.; Jerome, R. *Macromolecules* 1996, 29, 3376.
- Ruokolainen, J.; Tanner, H.; ten Brinke, G. *Macromolecules* 1995, 28, 7779.
- Lehn, J. M. *Supramolecular Chemistry*; Weinheim: VCH, 1995.
- Kato, T.; Hirota, N.; Fujishima, A.; Frechet, J. M. J. *Polym Prep Jpn* 1990, 39, 1950.
- Kato, T.; Hirota, N.; Fujishima, A. *J Polym Sci Part A Polym Chem* 1996, 34, 57.
- Stewart, D.; Imrie, T. C. *Macromolecules* 1997, 30, 877.
- Kumar, U.; Frechet, J. M. J.; Kato, T.; Ujiie, S.; Iimura, K. *Angew Chem Int Ed Engl* 1992, 31, 1531.
- Kihara, H.; Kato, T.; Uryu, T.; Frechet, J. M. J. *Liq Cryst* 1997, 24, 413.
- Bobrovsky, A. Yu.; Boiko, N. I.; Shibaev, V. P. *Polym Sci Ser A* 1997, 39, 798.
- Barmatov, E. B.; Bobrovsky, A. Yu.; Barmatova, M. V.; Shibaev, V. P. *Polym Sci Ser A* 1998, 40, 1077.
- Freidzon, Ya. S.; Boiko, N. I.; Shibaev, V. P.; Plate, N. A. *Vysokomol Soedin Ser A* 1987, 29, 934.
- Bobrovsky, A. Yu.; Boiko, N. I.; Shibaev, V. P. *Liq Cryst* 1998, 24, 489.
- Shibaev, V. P.; Lam, L. *Liquid Crystalline and Mesomorphic Polymers*; Springer: New York, 1996.
- Kostromin, S. G.; Talroze, R. V.; Shibaev, V. P.; Plate, N. A. *Makromol Chem Rapid Commun* 1982, 3, 803.
- Joesten, M. D.; Schaad, L. J. *Hydrogen Bonding*; Dekker: New York, 1974.
- Freidzon, Ya. S.; Boiko, N. I.; Shibaev, V. P.; Plate, N. A. *Vysokomol Soedin Ser A* 1987, 29, 464.
- Adams, J. E.; Haase, W. *Mol Cryst Liq Cryst* 1971, 15, 27.
- Bak, C. S.; Labes, M. M. *J Chem Phys* 1975, 63, 805.
- Chilaya, G. S.; Lisetskii, L. N. *Usp Fiz Nauk* 1981, 134, 279.
- Shibaev, V. P.; Freidzon, Ya. S. In *Side Chain Liquid Crystal Polymers*; Chapman & Hall: New York, 1989.
- Finkelmann, H.; Rehage, G. *Makromol Chem Rapid Commun* 1980, 1, 733.